Electronic Supplementary Material (ESI) for Journal of Materials Chemistry A.

Highly stable lithium-sulfur batteries based on p-n heterojuctions embedded on hollow sheath carbon propelling polysulfides conversion

Han Zhang,[a] Zongbin Zhao,[,a] Ya-Nan Hou,[a] Yongchao Tang,[a] Jingjing Liang,[a] Xuguang Liu,[b] Zhichao Zhang,[c] Xuzhen Wang[a,c] and Jieshan Qiu*[,a]*

[a] State Key Lab of Fine Chemicals, Liaoning Key Lab for Energy Materials and Chemical Engineering, PSU-DUT Joint Center for Energy Research, School of Chemical Engineering, Dalian University of Technology, Dalian 116024, China.

[b] Key Lab of Interface Science and Engineering in Advanced Materials, Ministry of Education, Taiyuan University of Technology, Taiyuan 030024, China

[c] School of Chemistry, Dalian University of Technology, Dalian 116024, China.

*E-mail addresses: zbzhao@dlut.edu.cn (Z. Zhao), jqiu@dlut.edu.cn (J. Qiu).

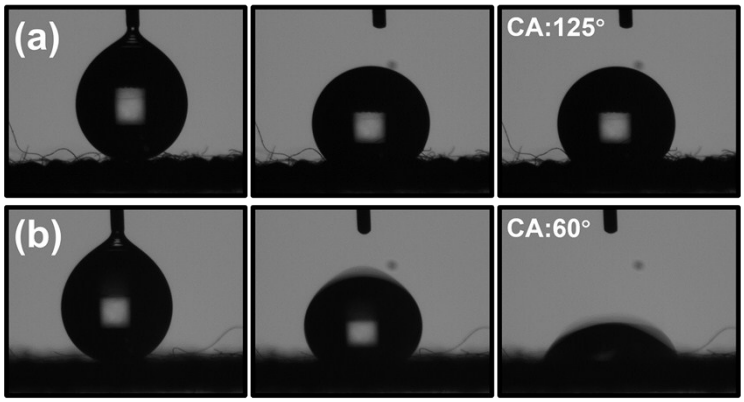

Fig. S1. Photographs of static water contact angle of (a) untreated-carbon cloth and (b) the carbon cloth of pre-treated by oxygen plasma.

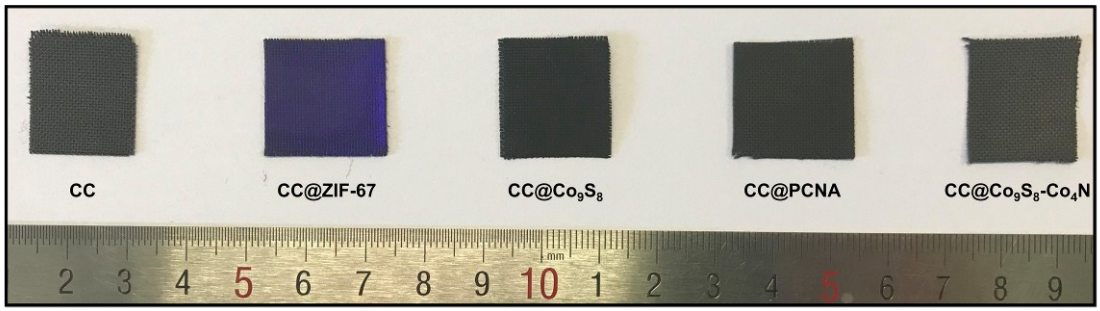

Fig. S2. A digital photograph of CC, CC@ZIF-67, CC@Co_9S_8, CC@PCNA and CC@Co_9S_8-Co_4N.

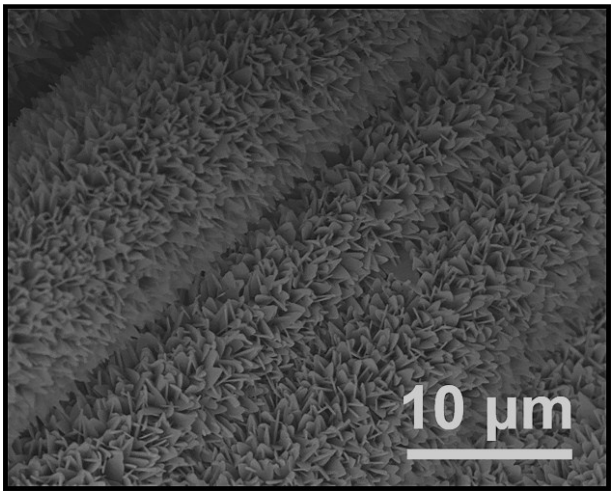

Fig. S3. Low-magnification FE-SEM image of CC@ZIF-67.

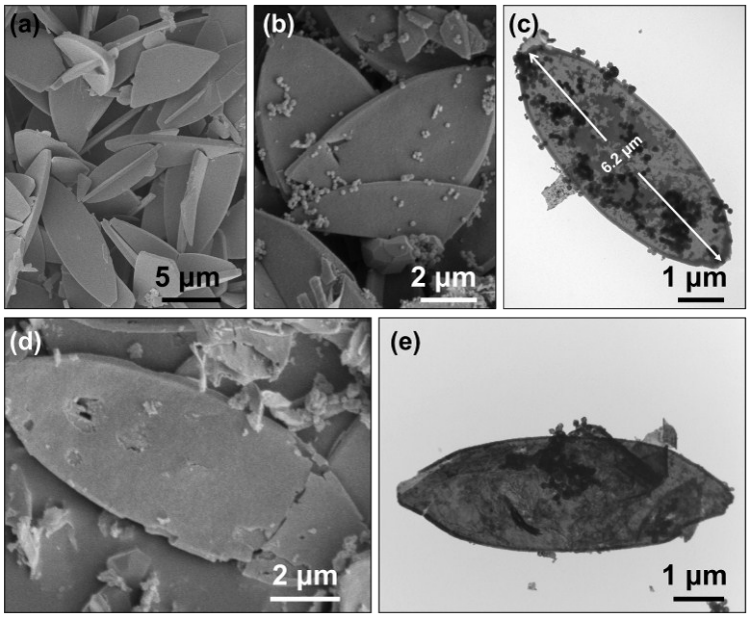

Fig. S4. FE-SEM images of (a) ZIF-67, (b) Co_9S_8 and (d) Co_9S_8-Co_4N. TEM images of (c) Co_9S_8 and (e) Co_9S_8-Co_4N

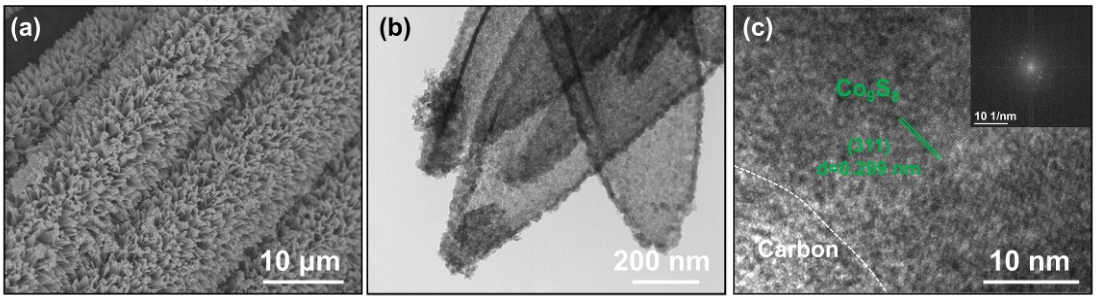

Fig. S5. (a) FE-SEM, (b) TEM and (c) HR-TEM images of CC@Co_9S_8.

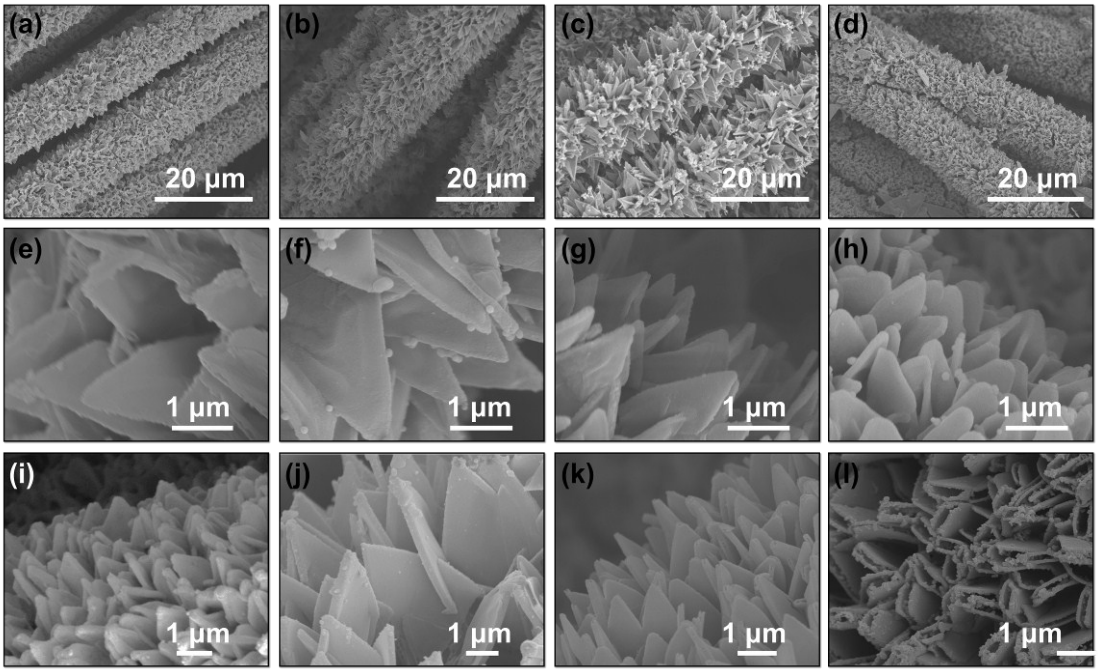

Fig. S6. The FE-SEM images show the formation of hollow structure after (a, e, i) 0.5 h, (b, f, j) 1 h, (c, g, k) 2 h and (d, h, l) 4 h of sulfidation reaction, respectively. The FE-SEM images of (a-h) after sulfidation reaction and (i-l) CC@Co_9S_8.

During the sulfidation reaction, a series of changes take place subsequently. Firstly, the surface of ZIF-67 form a layer of Co-based sulfides by the S^{2-} produced from TAA to react with Co ions. The thin shell can confine the further contact between the S^{2-} and internal Co ions. Secondly, compared with S^{2-} (184 pm), the Co ions (74 pm) has smaller ionic radius. With a mechanism similar to the Kirkendall effect, the internal Co ions released from ZIF-67 can penetrated the shell layer of sulfides to continue the reaction with external sulfur ions, resulting in the formation of a hollow structure.

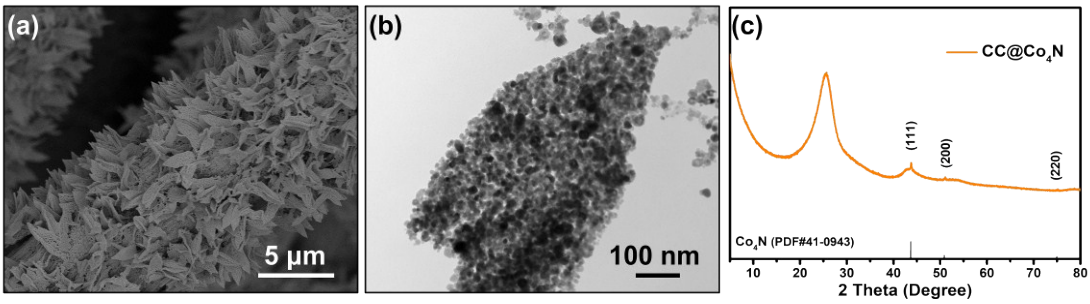

Fig. S7. (a) FE-SEM images, (b) TEM images and (c) XRD patterns of CC@Co_4N.

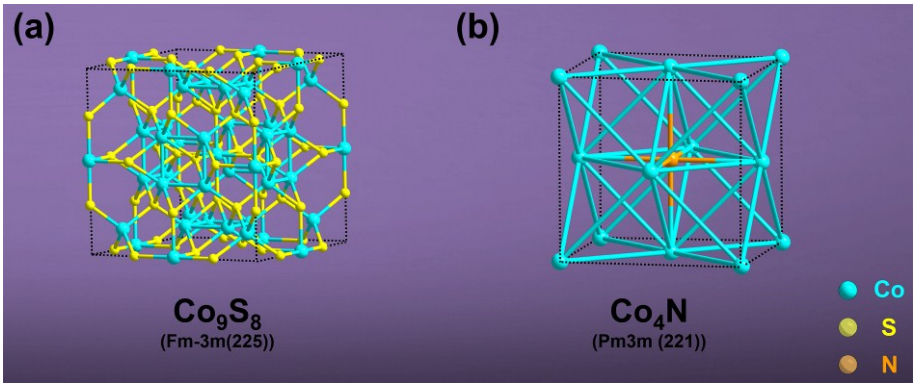

Fig. S8. Unit cells of Co_9S_8 and Co_4N structures.

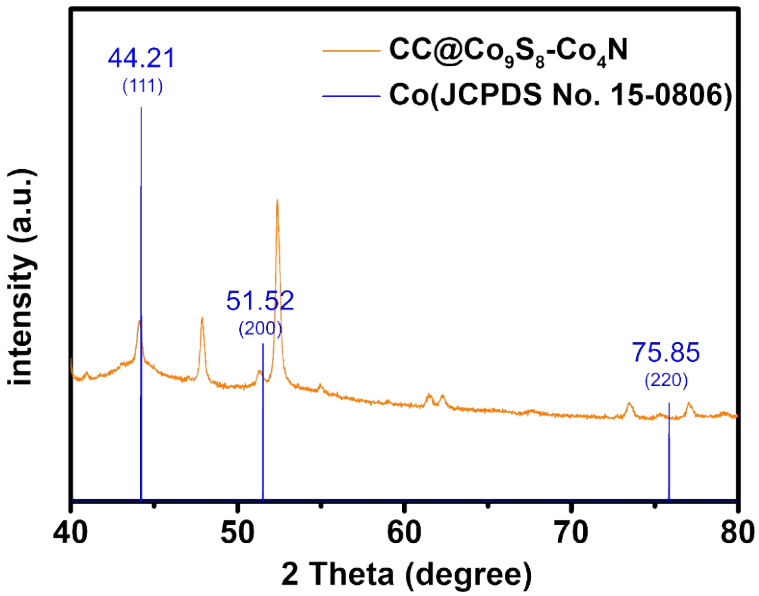

Fig. S9. XRD patterns of Co and CC@Co_9S_8-Co_4N. The standard XRD pattern for fcc Co (JCPDS No. 15-0806).

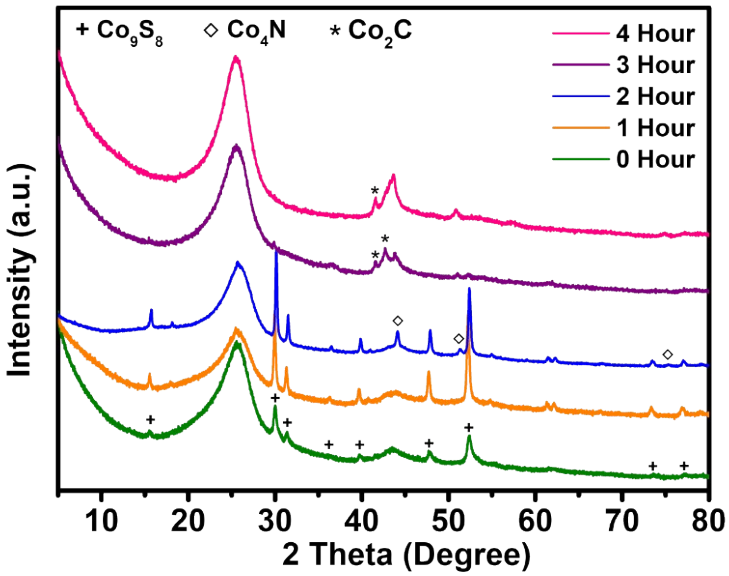

Fig. S10. The XRD patterns of Co-based compounds obtained at different nitridation time (0, 1, 2, 3 and 4 h).

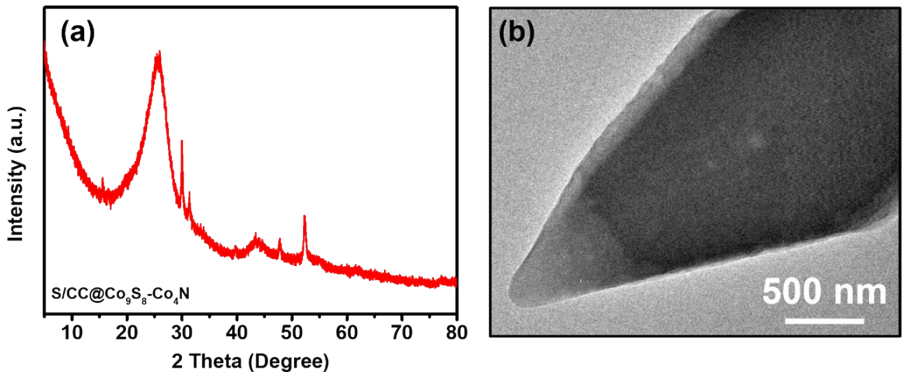

Fig. S11. (a) XRD pattern of S/CC@Co_9S_8-Co_4N, (b) TEM image of S/CC@Co_9S_8-Co_4N.

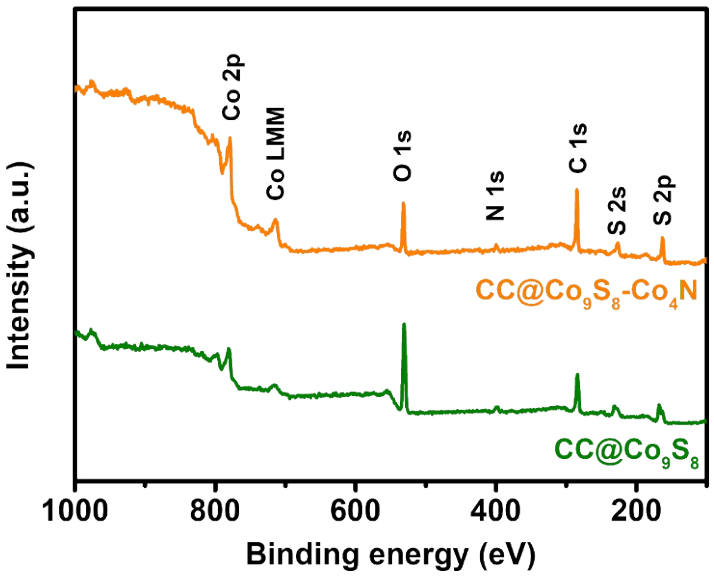

Fig. S12. XPS survey spectra of CC@Co_9S_8 and CC@Co_9S_8-Co_4N.

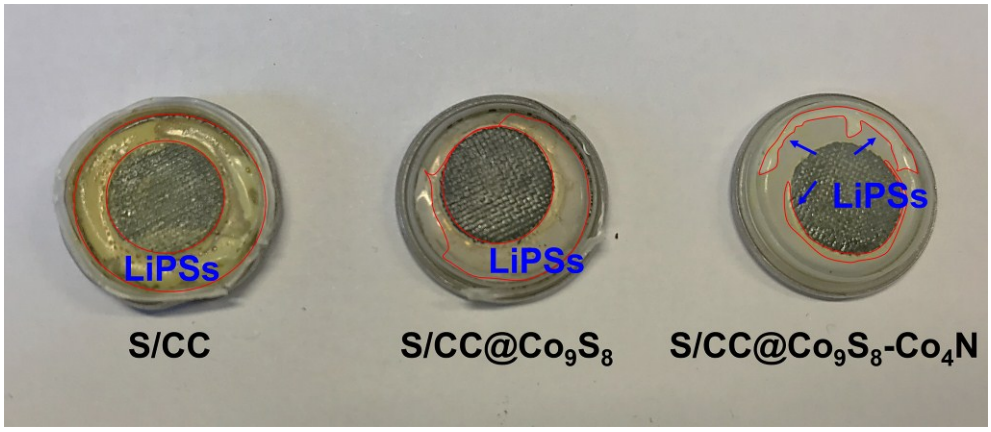

Fig. S13. Digital photo of cycled separators of S/CC, S/CC@Co_9S_8 and S/CC@Co_9S_8-Co_4N.

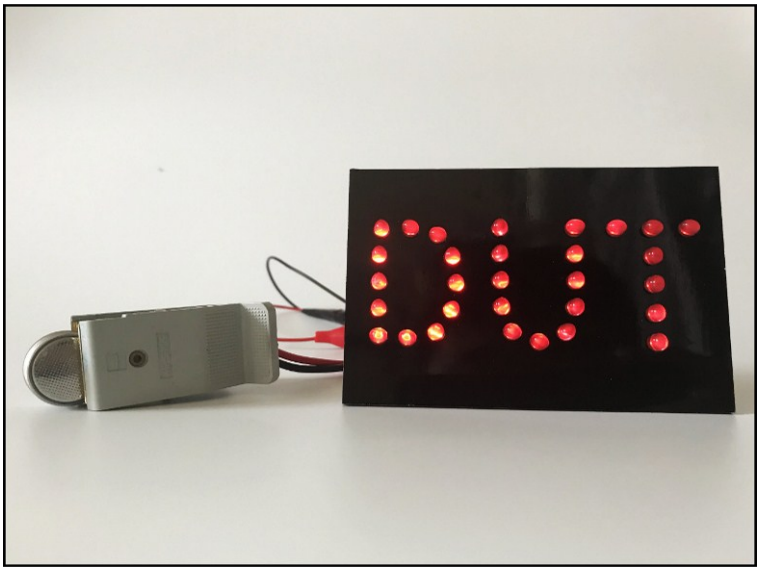

Fig. S14. Digital photo that shows the lithium-sulfur batteries powering 30 LED device.

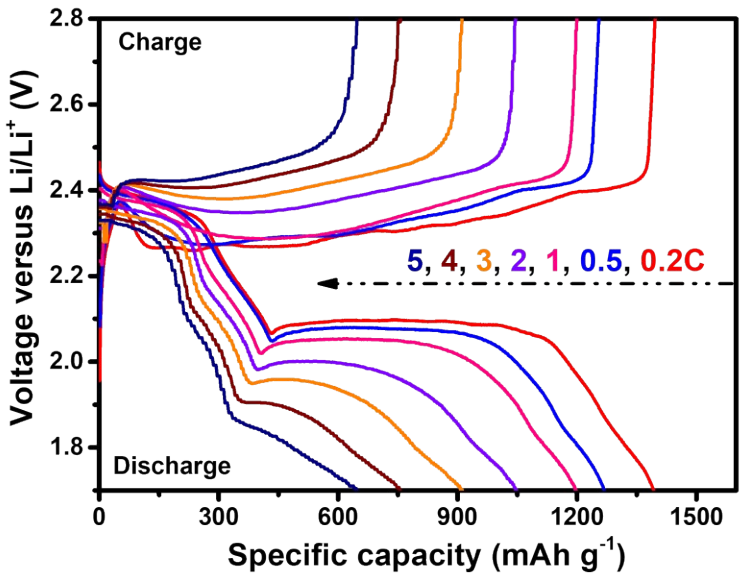

Fig. S15. Galvanostatic charge/discharge curves at current rate of 0.2, 0.5, 1, 2, 3, 4 and 5 C tested between 1.7~2.8 V of S/CC@Co_9S_8-Co_4N.

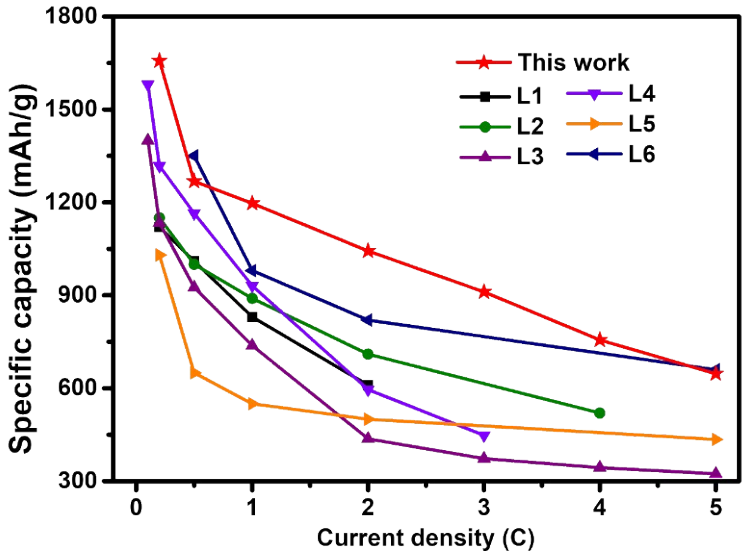

Fig. S16. A comparison of S/CC@Co_9S_8-Co_4N heterostructure with recently reported carbon cloth/fiber cathode materials in Lithium-sulfur batteries. (L1: Co_3O_4 nanoneedle array on carbon cloth,[1] L2: mesoporous SnO_2 nanosheets on carbon nanofibers,[2] L3: TiO_2 nanowires on carbon cloth,[3] L4: WS_2 nanosheets on carbon cloth,[4] L5: TiO_2 wrapping layer on carbon fiber,[5] L6: TiO_2-grafted carbon paper[6]).

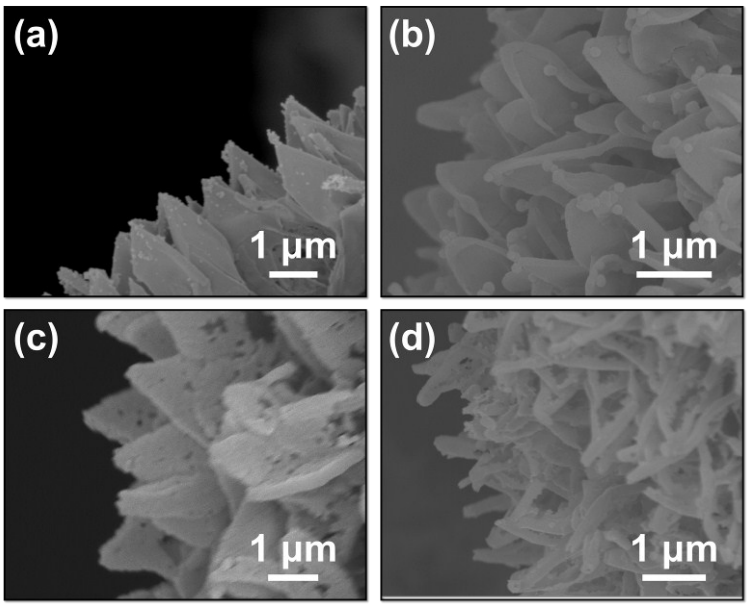

Fig. S17. FE-SEM images of CC@Co_9S_8-Co_4N show the different sulfidation reaction after (a) 0.5, (b) 1, (c) 2 and (d) 4 h.

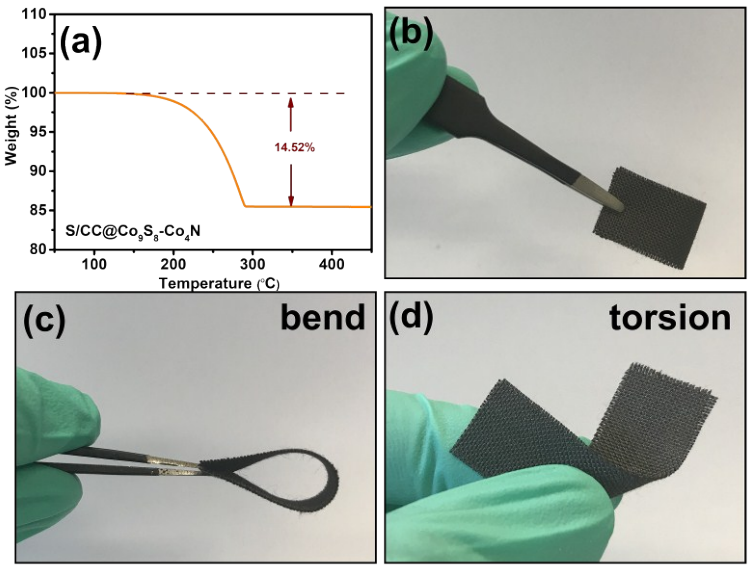

Fig. S18. (a) TGA curve of S/CC@Co_9S_8-Co_4N. (b-d) Digital images of the bend and torsion states of the S/CC@Co_9S_8-Co_4N.

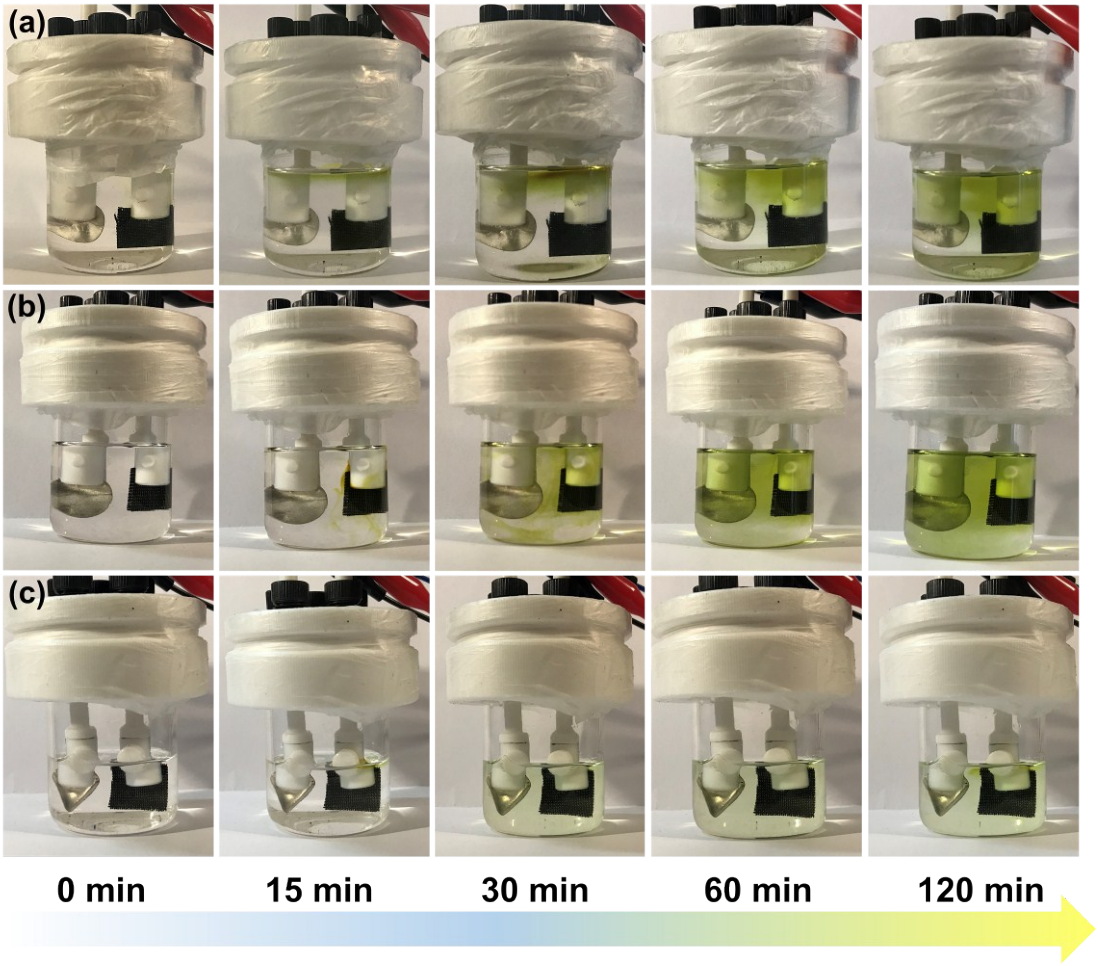

Fig. S19. Visual illustration of polysulfide entrapment of (a) S/CC@Co_9S_8, (b) S/CC and (c) S/CC@Co_9S_8-Co_4N composites.

Tab. S1. Co content and quantitative elemental analysis of the CC@Co_9S_8 and CC@Co_9S_8-Co_4N.

Sample	Icp	Element				
	Co(%)	C(wt%)	H(wt%)	N(wt%)	S(wt%)	O(wt%)
CC@Co_9S_8	5.41	73.63	0.23	1.25	19.86	0.05
CC@Co_9S_8-Co_4N	4.50	71.41	5.33	2.53	12.96	0.07

Tab. S2. Performance comparison of CC@Co_9S_8-Co_4N with other representative sulfur host materials for Li-S batteries in the literatures.

Ref.	Sulfur host materials	Sulfur loading in electrodes (mg cm^{-2})	Current density (1C=1675 mAh g^{-1})	Cycle number	Decay per cycle
This work	**S/CC@Co_9S_8-Co_4N**	**1.4~2.0**	**1 C**	**1000**	**0.030%**
		1.4~2.0	**5 C**	**1000**	**0.027%**
		6.1	**0.2 C**	**200**	**0.084%**
Ref. S2	C@SnO_2/S	2.0	2 C	1000	0.024%
Ref. S3	CC/TiO_2/S	1.5~2.0	1 C	700	0.045%
Ref. S5	TiO_2-ACF	3.2	0.2 C	100	0.023%
Ref. S6	CP@TiO_2-S	2.0	1 C	500	0.11%
Ref. S7	Co_9S_8–Celgard	2.0	1 C	1000	0.041%
Ref. S8	Co_4N/S	1.5~2.0	2 C	300	0.01%
Ref. S9	S@Co/N-PCNSs	0.8~1.0	5 C	400	0.036%
Ref. S10	Activated CNF Sheets	2.4	C/3	500	0.088%
Ref. S11	GOPAA	0.8	0.5 C	100	0.22%

Tab. S3. The relative parameters of S/CC@Co_9S_8-Co_4N at different current densities from 0.2 C to 5 C.

	m_s/mg	C_s/mAh g^{-1}	C_e/mAh g^{-1}	I/mA	V/v	E_m/Wh kg^{-1}	P_m/W kg^{-1}
0.2C	1.41	1657	230	0.47	2.10	342	700
0.5C	1.41	1268	176	1.18	2.08	259	1740
1 C	1.41	1197	166	2.36	2.05	241	3431
2 C	1.41	1043	145	4.72	2.00	205	6695
3 C	1.41	911	126	7.08	1.95	174	9791
4 C	1.41	756	105	9.44	1.90	141	12720
5 C	1.41	647	90	11.8	1.86	118	15565

m_s: the mass of cathode electrodes with the diameter of 10 mm;

C_s: the discharge capacity in the different current densities of sulfur;

C_e: the discharge capacity in the different current densities of cathode;

I: the charge/discharge current of electrodes;

V: average voltage of discharge;

E_m: specific energy density;

P_m: specific power density.

Note that specific energy density (E_m) and power density (P_m) are calculated by the following equations: $E_m = V \times C_e / m_s$, $Pm = I \times V / m_s$**, C is the discharge capacity at different rates in Fig. 5c.**

References

S1 Z. Chang, H. Dou, B. Ding, J. Wang, Y. Wang, X. Hao, D. R. MacFarlane, *J. Mater. Chem. A,* 2017, **5**, 250.

S2 M. Wang, L. Fan, X. Wu, D. Tian, J. Cheng, Y. Qiu, H. Wu, B. Guan, N. Zhang, K. Sun, Y. Wang, *J. Mater. Chem. A,* 2017, **5**, 19613.

S3 T. Lei, Y. Xie, X. Wang, S. Miao, J. Xiong, C. Yan, *Small*, 2017, **13**, 1701013.

S4 T. Lei, W. Chen, J. Huang, C. Yan, H. Sun, C. Wang, W. Zhang, Y. Li, J. Xiong, *Adv. Energy Mater.,* 2017, **7**, 1601843.

S5 K. Y. Xie, K. Zhang, Y. Z. Han, K. Yuan, Q. Song, J. G. Wang, C. Shen, X. R. Liu, B. Q. Wei, *Electrochim. Acta*, 2016, **210**, 415.

S6 Z. Zhang, Q. Li, K. Zhang, W. Chen, Y. Lai, J. Li, *J. Power Sources*, 2015, **290**, 159.

S7 J. He, Y. Chen and A. Manthiram, *Energy Environ. Sci*, 2018, **11**, 2560-2568.

S8 D. R. Deng, F. Xue, Y. J. Jia, J. C. Ye, C. D. Bai, M. S. Zheng and Q. F. Dong, *ACS Nano*, 2017, **11**, 6031-6039.

S9 S. Liu, J. Li, X. Yan, Q. Su, Y. Lu, J. Qiu, Z. Wang, X. Lin, J. Huang, R. Liu, B. Zheng, L. Chen, R. Fu and D. Wu, *Adv. Mater.*, 2018, **30**, 1706895.

S10 L. Qie, C. Zu and A. Manthiram, *Adv. Energy Mater.*, 2016, **6**, 1502459.

S11 G. Xu, Q.-b. Yan, A. Kushima, X. Zhang, J. Pan and J. Li, *Nano Energy*, 2017, **31**, 568-574.